Preserving the Acoustic Quality of Traditional Sasando with Optical Pickup and Biquad Filters

Team 182, Problem A

Abstract

This paper presents a method for reproducing the authentic acoustic sound of a traditional sasando instrument for its electric counterpart. The study assumed a gong-type sasando with a closed bamboo tube and one string per bridge. Three types of pickups, magnetic, piezoelectric, and optical, were investigated and compared on the basis of preservation of tone, sensitivity, noise immunity, and invasiveness. Optical pickups were determined to be the most optimal, being displacement-sensitive with minimal interference. The string motion was derived from the one-dimensional wave equation under fixed boundary conditions to determine the optimal pickup location. Analysis shows that the pickup should be placed as close to the bridge as possible to preserve clarity in tone and greater headroom. To emulate the natural resonance of the leaf resonator, a digital biquad band-pass filter with constant 0 db peak gain was designed, with cutoff frequencies of 98 Hz and 1047 Hz. The resulting coefficients for the biquad transfer function were $b = [0.059, 0.0, -0.059]$ and $a = [1.0, -1.9, 0.88]$. Resonances of the 70 cm closed bamboo tube within the leaf resonance range were modeled with harmonics at 245 Hz, 490 Hz, 735 Hz, and 980 Hz. The quality factor of the bamboo tube were calculated to be 19 ± 2 from the internal friction of $\tan\delta = 0.053 \pm 0.005$. Corresponding band-pass filters were determined to reproduce the combined resonance profile. Three types of amplifiers were looked into and comparisons show that Class AB type amplifier was selected for having the highest efficiency. The final system including optical pickups place immediate below the bridge, digital biquad band-pass filters, Class AB amplifier, and a moving-coil loudspeaker successfully retains the amplified range of the leaf resonator and reproduces the authentic acoustic sound of a traditional sasando.

Contents

1 Introduction

1.1 Background

The sasando is a stringed musical instrument native to the Rote Island of East Nusa Tenggara, Indonesia. The instrument consists of a bamboo tube with strings stretched along its length. Traditionally, the dried leaves of a lontar are woven into a semicircular, shell-like shape and to form an external resonator to that amplifies the musical sounds. The earliest versions of the sasando only had a few strings, but over time, the number of strings increased to reach a wider range of octaves (Tukan, Ceunfin, & Kian, 2020).

The growing need for a greater and more even amplification of sound brought forth the idea of designing an electric sasando (Bakok, 2014). This electric version replaces the leaf resonator with electronic pickups and an amplifier, causing a loss in the original warm acoustic tone of this traditional instrument.

1.2 Problem Restatement

The goal of this problem is to develop a method that enables the electronic sasando to reproduce the authentic acoustic sound of a traditional sasando, which has a bamboo tube that is 70 cm in length and 8 cm in diameter. The electric sasando replaced the traditional external resonator of the acoustic sasando with a pickup and speaker. The design and configuration of the electronic pickup and amplification system must be selected to preserve the acoustic tone and account for the natural amplification of the traditional resonator for frequencies between 98 Hz and 1047 Hz.

2 Assumptions

2.1 Sasando Type and Structure

For this analysis, it is assumed that the sasando sound being replicated is of the gong sasando, as it is the earliest and of the simpliest form. The structure of the sasando is also assumed to be a tube closed on both ends with only one string on each bridge.

It is also assumed that only the sections of the strings below the bridge is played, as documented playing techniques and and visual observation from performances have not suggested otherwise.

2.2 Boundary Condition for Strings

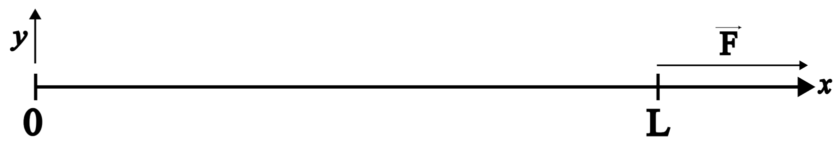

Figure 1: Coordinate system of a string.
Note. Adapted from from *The science of electric guitars and guitar electronics*, by J. Lähdevaara (2012), Books On Demand. (OCLC: 861737010)f

Note that the x-axis in the coordinate system is only parallel to the string itself but not the ground.

The string is fixed at $x = 0$ and $x = L$, and vibrational motion is only present for $0 \leq x \leq L$. The bridge is located at 0 and L is the lower end of the sasando.

Define the transverse displacement $y(x, t)$ on $[0, L]$. The boundary conditions are

$$y(0, t) = 0, \qquad y(L, t) = 0.$$

2.3 String Condition Assumptions

1. The string is perfectly flexible without internal energy loss.
2. Both endpoints are fixed and perfectly rigid (no boundary energy loss).
3. The horizontal force F in Figure 1 is constant at all times.
4. The motion of the string is restricted to a 2D plane.
5. The string has a uniform density.
6. Frictions and gravitational forces are neglected.

3 Notations

The main notations used throughout this paper are defined in this section in the order that they appear. More specific symbols and variables will be introduced and explained contextually when they become relevant.

Symbol	Description
L	Length of the playable range on a string
A_n	nth order resonance frequency amplitude
ν	Transverse velocity of wave function
C	Capacitance
A	Area
f	Frequency
ε_0	Permittivity of free space
p	Position of string being plucked
ρ	Density of the string
μ	Linear mass density of the string
P	The location of pickup
f_0	Center frequency
Q	Quality factor
ω_0	Normalized angular frequency of the filter
α	Ratio of the bandwidth relative to the center frequency

4 Pickup Selection

4.1 Background

An electronic pickup is an important element that acts as a sensor of the motion of strings and a transducer of that motion into electric signals in typical string instruments (Lähdevaara, 2012). The electric signal could then be used to generate the corresponding amplified tone (Lähdevaara, 2012). Depending on the types of pickup, they are sensitive to displacement or velocity inputs. Below we explore and consider three main types of pickup: magnetic, optical, and piezoelectric pickup.

4.2 Magnetic Pickups

Magnetic pickup is the most common pickup by far on musical electric instruments, i.e. electric guitars. The pickups are usually built around cylindrical permanent magnets, including Alnico and ferrite magnets. In result a moderately strong magnetic field, $\vec{B}$ averaging around 0.1 T is produced, which would readily react with strings made by ferromagnetic materials (Lähdevaara, 2012). The strings become magnetized, and their dipole moments $\vec{\mu}$ become aligned with the direction of $\vec{B}$ to form a larger magnetic unit (Lähdevaara, 2012). A schematic model of the magnetic fields for both the cylindrical magnet and the string is shown in Figure 2.

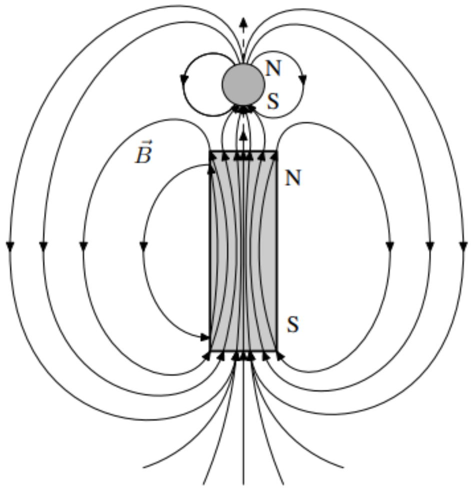

Figure 2: A combined magnetic unit of both the magnetized string and the cylindrical magnet.
Note. Reprinted from *The science of electric guitars and guitar electronics*, by J. Lähdevaara (2012), Books On Demand. (OCLC: 861737010)

When a string is plucked, it causes a distortion of $\vec{B}$, which in turn generates a current and induced emf, ϵ, by Faraday's law of Induction (Red Lion Controls, 2000).

$$\epsilon = -N\frac{d\Phi_B}{dt}$$

where N is the number of turns in the coil and the magnetic flux is related to the magnetic field of the pickup magnet $\vec{B}$:

$$\Phi_B = \int \vec{B} \cdot \mathrm{d}\vec{S}$$

where S represents the surface area enclosed by the pickup winding.

A typical magnetic pickup in a guitar, for example, would consist of a linear array of about six cylindrical magnets wound with a copper wire coil (usually more than 6000 turns), as shown in Figure 3.

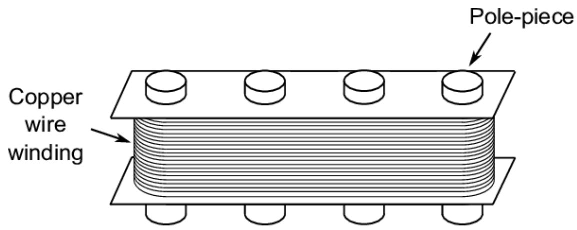

Figure 3: The components for a single magnetic pickup: the copper wire coil surrounding an array of cylindrical magnets.
Note. Reprinted from *Proceedings of the International Symposium on Musical Acoustics (ISMA 2014)*, Mustonen, M., Kartofelev, D., Stulov, A., & Välimäki, V. (2014, July). *Experimental verification of pickup nonlinearity.*

The magnitude of the voltage signal is dependent on the speed of approach of the string as the magnetic flux rate of change is directly related to the frequency of the string's vibration (Lähdevaara, 2012). Thus magnetic pickups are considered to be velocity-sensitive pickups (Red Lion Controls, 2000). The characteristic of using a velocity-sensitive pickup can be seen from differentiating the displacement function defined at Equation (14) with respect to time, which would yield

$$\frac{\partial y(x,t)}{\partial t} = -\sum_{n=1}^{\infty} \frac{\sqrt{\nu} n\pi A_n}{L} sin(\frac{n\pi x}{L}) sin(\frac{\sqrt{\nu} n\pi t}{L}) \tag{1}$$

The more detailed derivation of the 1D displacement wave function could be found later in Section 5.1.3.

It could be seen using this relationship that with the **n* multiple the higher spectral harmonics would take dominance, implying that higher order harmonics would be more dominant than they are in a natural acoustic oscillation, giving electric instruments using magnetic pickups a different, often sharper tone (Horton, 2009).

4.3 Piezoelectric Pickups

Piezoelectric pickups are an alternative transducer type for semi-acoustic and electric guitars. They are often used for fitting existing musical instruments, mostly stringed ones with a cavity, and give them electric properties. Unlike magnetic pickups, piezoelectric pickups rely on the piezoelectric effect, where crystalline materials generate electric voltage when mechanically stressed (Bera, 2016). This principle is based on the linear relationship between the applied force and the induced polarization produced by crystals lacking a center of symmetry (Gautschi, 2002) as seen in Figure 4.

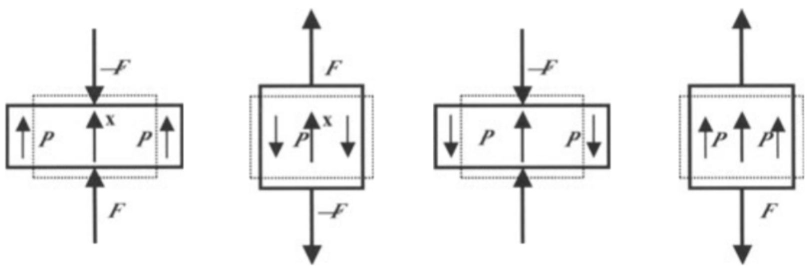

Figure 4: The direct piezoelectric effect.
Note. Adapted from *Piezoelectric Sensorics*, by G. Gautschi, 2002, Springer. Retrieved from http://link.springer.com/10.1007/978-3-662-04732-3

This linear relation can be represented by combination of the equations:

$$D = dT + \varepsilon_0 E$$
$$S = sT + d^t E$$

where D is the electric flux density, ε is the permittivity of space, E is the electric field strength, S is the linearize strain, s is the stiffness, T is the stress, and d is the piezoelectric tensor.

A typical piezoelectric pickup for a guitar, placed under the saddle can be seen in Figure 5. The pickup is placed in direct contact with the strings, so when a string is plucked, the bridge transmits pressure variations that produce and electric voltage proportional to the instantaneous string displacement (Lähdevaara, 2012). For this reason, piezoelectric pickups are considered displacement-sensitive as their output depends on physical displacement of the strings rather than the rate of change.

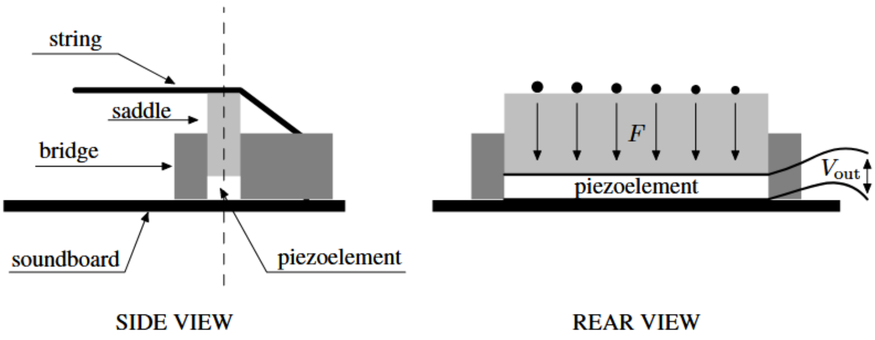

Figure 5: Composition of an under-saddle piezoelectric pickup
Note. Reprinted from *The science of electric guitars and guitar electronics*, by J. Lähdevaara (2012), Books On Demand. (OCLC: 861737010)

The electric signal generated by a piezoelectric pickup usually exhibits high output impedance due to the nature of the crystalline material to act as a capacitor (Lähdevaara, 2012). As external forces deform the crystalline material, the internal charges are displaced, resulting in a net surface charge and producing voltage across the electrodes. This displacement across the dielectric is what gives the piezoelectric crystals their capacitative behaviour.

The capacitance of the piezoelectric crystal can be calculated using:

$$C = \frac{\varepsilon_r \varepsilon_0 A}{d}$$

where ε_r is the relative permittivity of the crystal and d is the thickness. Since the area of the dielectric is small compared to the thickness, the piezoelectric crystal has very small capacitance.

The relationship between the impedance of a capacitor, the capacitance, and the frequency of the signal is given by the equation:

$$Z = \frac{1}{2\pi f C}$$

where Z is the impedance. From this it can be seen that since the impedance is inversely proportional to the capacitance, the piezoelectric pickup would have high output impedance due to its low capacitance. This means that the low input impedance of a typical amplifier would distort the frequency response and thus, an additional preamplifier buffer would be needed to maintain the full range from a piezoelectric pickup (Lähdevaara, 2012).

4.3.1 Piezoelectric Bimorph Pickups

A special type of piezoelectric pickups are the piezoelectric bimorph pickups. These are the most commonly chosen pickup to be used for bowed instruments such as violin and cello. Unlike typical piezoelectric pickups, bimorph pickups consists of two layers of piezoelectric material rather than one, with a thin metallic sheet between them as seen in Figure 6.

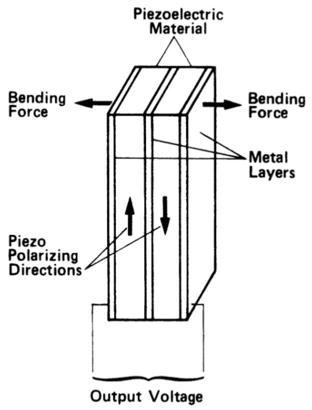

Figure 6: Components of a piezoelectric bimorph pickup.
Note. Reprinted from *Pickups for the vibrations of violin and guitar strings using piezoelectric bimorphic bender elements* (Tech. Rep.), by M. V. Mathews, 1988, Stanford University, Center for Computer Research in Music and Acoustics (CCRMA).

Instead of being placed as a layer beneath the bridge, this pickup is inserted into the bridge itself as seen in Figure 7. In this way, the vibration of the strings bend the pickup, compressing one layer and stretching the other. This produces opposite polarizing directions, generating an increase in output voltage and improving sensitivity (Mathews, 1988).

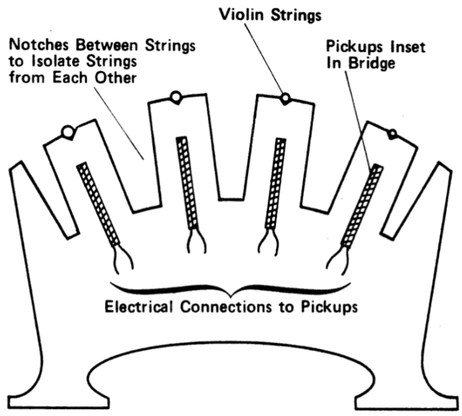

Figure 7: Composition of a violin bridge with piezoelectric bimorph pickups.
Note. Reprinted from *Pickups for the vibrations of violin and guitar strings using piezoelectric bimorphic bender elements* (Tech. Rep.), by M. V. Mathews, 1988, Stanford University, Center for Computer Research in Music and Acoustics (CCRMA)

4.4 Optical Pickups

Optical pickups consist of a rather simplistic coupled system. At least one light source and one photodetector are placed on either side of a string, where vibration of the string would create a difference in light intensity captured by the photodetector (Kubilary, 2018). The difference in light intensity would be transduced into a voltage signal that produces the corresponding amplified tone (Kubilary, 2018). The most common type of photodetector used is a photodiode, using LED as the light source. In most scenarios the use of a light source like infrared LEDs would generate a relatively weak signal due to weak light intensity. Thus, a pre-amp circuit must be coupled along with the photodiode to amplify the voltage signal enough for transmitting to a power amplifier, avoiding distortion and noise (ElProCus, n.d.). Such a system is referred to as a phototransistor.

A photointerrupter is created by combining a gallium infrared light emitting diode (IR LED) with a phototransistor (Lähdevaara, 2012). A figure of the system is shown in Figure 8. A standard positioning of the string is such that when it is not vibrating, half of the beam is blocked. An experiment conducted by Hanson with optical pickups demonstrated that there is a negative linear relationship between the displacement of the string and the base voltage signal (Hanson, 1987). Thus, the optical pickup is determined to be a displacement sensitive pickup.

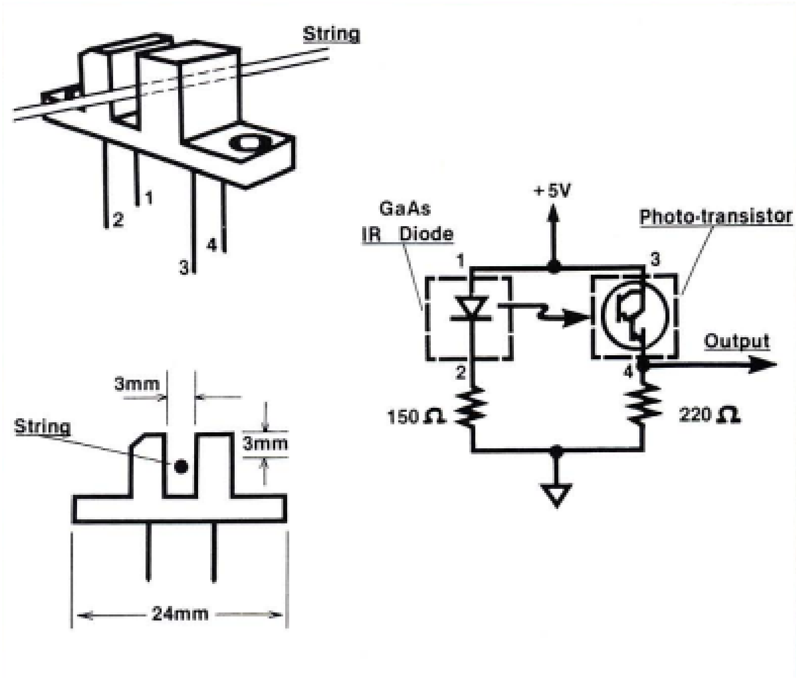

Figure 8: Photointerrupter module (H21B1) with string position. A labeled circuit for the module is also shown, where the dashed lines imply components of the module
Note. Reprinted from *The Physics Teacher*, Hanson, R. J. (1987). Optoelectronic detection of string vibration, 25, 165–166.

Similar to piezoelectric pickups which are also displacement-sensitive, the fundamental frequency is most dominant for optical pickups. High order harmonics typically get cut off from the spectrum due to the fast-decaying term of the amplitude, A_n. The displacement equation that is related to the voltage signal output is defined as:

$$y(x,t) = \sum_{n=1}^{\infty} A_n \cos(\frac{\sqrt{\nu} n\pi}{L} t) \sin(\frac{n\pi x}{L}) \tag{2}$$

Note: Detailed derivations of the wave equation can be found in Section 5.1.3.

A visual graph of the spectrum produced with optical pickup at a certain pluck position and pickup position is shown in Figure 9. It could be seen that the upper partials, specifically the fundamental frequency has dominance in amplitude. From this observation one can deduce that optical pickups tend to bring sound and tone closer to natural acoustics.

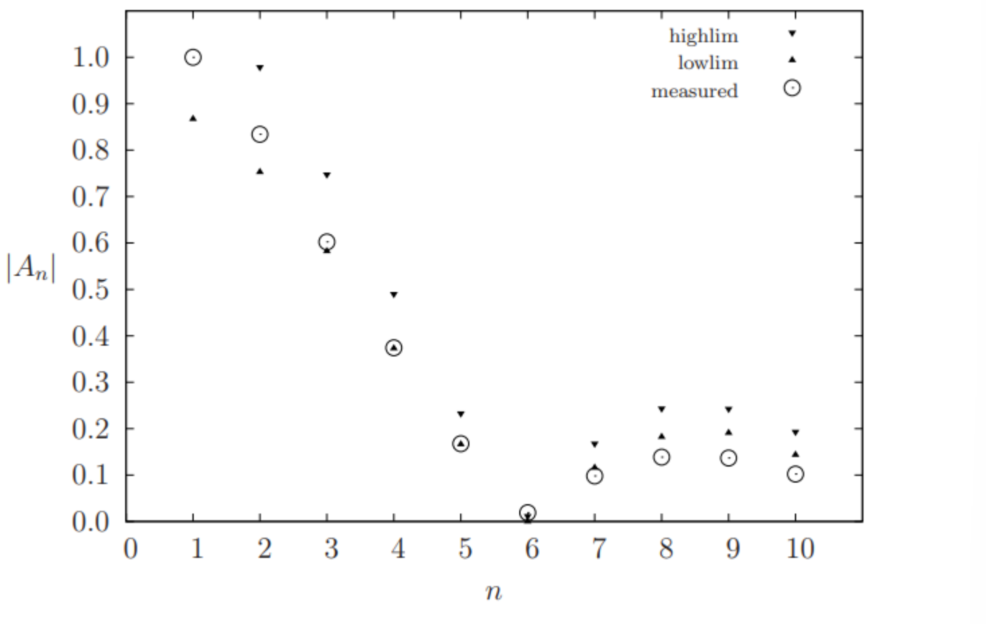

Figure 9: Amplitude Spectrum from a pluck position of $p = \frac{L}{6}$ and pickup position of $P = 8$ mm from left boundary.
Note. Adapted from *The science of electric guitars and guitar electronics*, by J. Lähdevaara (2012), Books On Demand. (OCLC: 861737010)

4.5 Comparison

The objective is to preserve the acoustic quality of a traditional sasando, thus a pickup must be chosen such that little alterations to the original tone quality is made. An optimal pickup should also offer an extensive range for materials of string, installation, and barrier to noises (often changing magnetic fields).

For instance, magnetic pickups are only functional when paired with metal strings, and single-coil pickups are subjected to the present external electromagnetic radiation arising from power transmission networks (Lähdevaara, 2012). The magnetic field contained in electromagnetic radiation changes in time, which would also induce an additional current on the pickup coil (Lähdevaara, 2012). Of course, there are present remedies to resolve this issue of "hum". A "humbucker" pickup is one of the many proposed designs to shield the pickup from the external noise of EM radiation. However, magnetic pickups in general are not considered in this setting, as the tone of the acoustics is altered due to their velocity-sensitive characteristic. As mentioned above, taking the derivative of the wave displacement function boosts the higher-order frequency amplitudes because of the decay term $\frac{1}{n}$ (an extra multiple of n in Equation (1)) instead of $\frac{1}{n^2}$ in Equation (2). A real-life example of such alterations could be seen in electric guitars, where higher pitches are more sharp and had a different tone quality compared to acoustic guitars. This defeats the goal of designing a model that produces tone as close to the acoustic quality of traditional sasandos as possible.

Both piezoelectric and optical pickups are examples of displacement-sensitive transducers, which greatly preserve the original tone quality of string acoustics. We then consider the installation and sound quality. Both pickup type are not influenced by external electromagnetic radiation, as they measure mechanical movements instead of changes in magnetic field (Lähdevaara, 2012). However, piezoelectric pickups are considered to be more "invasive" than the other, primarily because the pickup needs to be installed under the bridge stud to measure the pressure caused by string vibration (Englert, 2018). This often implies drilling into the bore of musical instruments, which is considered to be a more invasive approach (Englert, 2018). Specifically for a sasando where the bridge location varies for each string, it is not ideal to install piezoelectric pickups as independent systems are required for each string. This would cause complications and there is also possibility that the piezoelectric pickup for each string would pick up vibrations from other strings through the bamboo tube.

Based on all the above considerations, optical pickups are most optimal to preserve the acoustic quality of a sasando. With the optical pickup, a separate photodetector-LED system would still be required to detect vibration for each string. However, the system is set up such that the interference and noise from other strings and the environment are minimized. The position of optical pickups are not limited to under the bridge, rather, they are placed on the surface in the proximity of the bridge in order to minimize noise and enhance acoustic property. Such arrangements would also imply a less invasive installation and flexible adjustment to location depending on need and tuning.

5 Pickup Location

5.1 The Wave Function of the String

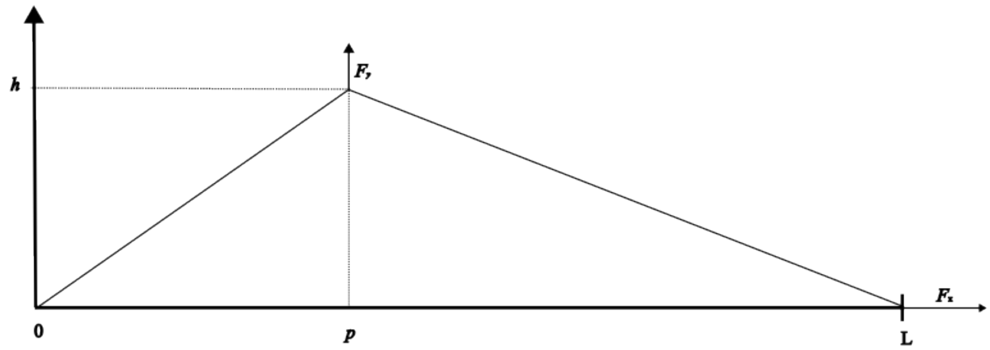

Figure 10: Geometry shape of a plucked string.
Note. Adapted from from *The science of electric guitars and guitar electronics*, by J. Lähdevaara (2012), Books On Demand. (OCLC: 861737010)

Figure 10 shows the geometry of a plucked string. $\vec{F}_x$ is the same force as $\vec{F}$ in Figure 1. The net force in this case is simply

$$\vec{F}_{net} = \vec{F}_x + \vec{F}_y$$

$$F_{net} = \sqrt{F_x^2 + F_y^2}$$

The slopes for the two segments of the string can be taken as $\frac{h}{p}$ and $\frac{h}{L-p}$. To look deeper into this, one could take a small segment of the deflected string and analyze the compound forces.

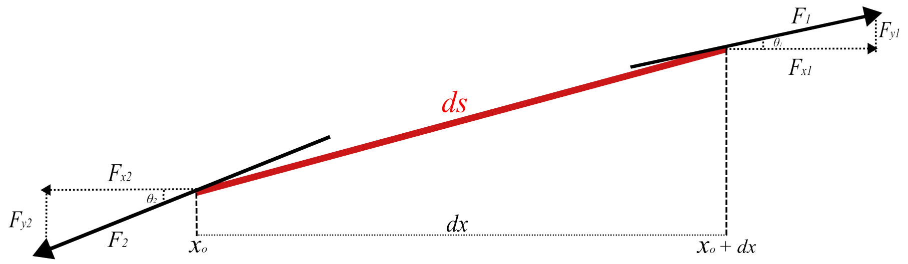

Figure 11: Force diagram of a small segment of string ds, where the mass for ds is dm. Note. Adapted from from *The science of electric guitars and guitar electronics*, by J. Lähdevaara (2012), Books On Demand. (OCLC: 861737010)

As mentioned in the presumption in Section 2.3 the tension is fixed across the entire string. Thus the tension forces in the above diagram holds the below equality

$$F_{x2} = F_{x1} = F_x$$

Both F_{y1} and F_{y2} can be expressed in terms of F_x:

$$F_{y1,2} = F_x \tan\theta_{1,2}$$

To make the string in motion, it has to break the equilibrium state. This means that forces in the y direction has to be asymmetric. One could then imply Newton's second law with the difference in F_y.

$$\begin{gathered} F_{y2} - F_{y1} = F_{net} \\ F_x \tan\theta_{x1} - F_x \tan\theta_{x2} = a \cdot dm \\ F_x\left(\frac{\partial y}{\partial x}\bigg|_{x0+dx} - \frac{\partial y}{\partial x}\bigg|_{x_o}\right) = a \cdot dm \end{gathered}$$

Since the bracketed term is the infinitesimal change over the first derivative, one could derive it into the second derivative using the operator $\frac{\partial}{\partial x}$.

$$F_x \frac{\partial}{\partial x}\left(\frac{\partial y}{\partial x}\right)dx = F_x \frac{\partial^2 y}{\partial x^2}dx = a \cdot dm$$

Substitute $dm = \rho dv = \rho A dx$, where A is the cross sectional area of the string:

$$\begin{gathered} F_x \frac{\partial^2 y}{\partial x^2}dx = \frac{\partial^2 y}{\partial t^2}\rho A dx \\ \frac{\partial^2 y}{\partial t^2} = \frac{F_x}{\rho A}\frac{\partial^2 y}{\partial x^2} \end{gathered}$$

It is known that the transverse wave velocity can be defined as

$$\nu = \frac{T}{\mu}$$

It should be obvious that the constant term in the previous equation is in fact the transverse wave velocity, as $m(x) = \mu x = \rho A x$ is linear mass function of the string.

$$\frac{\partial^2 y}{\partial t^2} = \nu \frac{\partial^2 y}{\partial x^2} \tag{3}$$

To solve the wave function, first assume that it is in the form of separable equation.

$$y(x,t) = F(x)G(t) \tag{4}$$

$$\frac{\partial^2 y}{\partial x^2} = F''G$$

$$\frac{\partial^2 y}{\partial t^2} = FG''$$

Substitute the first and second derivatives back in Equation 3.

$$FG'' = \nu F''G$$

$$\frac{G''}{\nu G} = \frac{F''}{F}$$

$$\frac{d^2G}{t^2}\frac{1}{\nu G} = \frac{d^2F}{dx^2}\frac{1}{F}$$

Set both sides of the equation equal to a constant k.

$$\frac{d^2G}{dt^2}\frac{1}{\nu G} = k \tag{5}$$

$$\frac{d^2F}{dx^2}\frac{1}{F} = k \tag{6}$$

From Section 2.2 it is assumed that the string is fixed at 0 and L. Substitute this condition into Equation (4) to build boundary conditions.

$$0 = y(0,t) = y(L,t) = F(0)G(t) = F(L)G(t)$$

By getting the first derivative of the above equation at the same time stamp t, it is noticeable that $F(x)$ has to be 0 at distance 0 and L.

$$F(0) = F(L) = 0 \tag{7}$$

5.1.1 Solving the Time Independent Differential Equation

There are three cases in total: $k < 0$, $k = 0$, and $k > 0$.

Calculations and intermediate steps for the last two cases will be briefly summarized here as their results are trivial.

When k = 0,

$$\frac{d^2F}{dx^2} = 0$$

thus $F = Ax + B$. After plugging in the boundary condition, $A = B = 0$.

When k > 0, take $F = e^{rx}$ and substitute it into Equation 6.

$$r^2 e^{rx} = ke^{rx}$$

thus $r = \pm\sqrt{k}$, and $F = Ae^{\sqrt{k}x} + Be^{-\sqrt{k}x}$. After plugging in the boundary condition, $A = B = 0$.

From the results from above, k has to be smaller than 0. Continue solving the differential equation at $k < 0$.

Let $k = -a^2$. Repeat the same procedure as when $k > 0$ and get $r = \pm ia$.

$$F_1 = e^{iax} = \cos ax + i \sin ax$$

$$F_2 = e^{-iax} = \cos ax - i \sin ax$$

Thus, by linear combination

$$\begin{aligned} F(x) &= AF_1 + BF_2 \\ &= A\cos ax + iA\sin ax + B\cos ax - iB\sin ax \\ &= (A+B)(\cos ax) + i(A-B)(\sin ax) \end{aligned}$$

Let $A + B = C_1$ and $i(A - B) = C_2$

$$F(x) = C_1 \cos ax + C_2 \sin ax \tag{8}$$

Plug in the boundary condition at $x = 0$,

$$0 = F(0) = C_1 cos(0) + C_2 sin(0)$$

Thus $C_1 = 0$. At $x = L$,

$$\begin{aligned} 0 &= F(L) = C_2 sin(aL) \\ 0 &= sin(aL) \\ aL &= n\pi \\ a &= \frac{n\pi}{L}\Bigg| \left\{ n \in \mathbb{Z}^+ \right\} \end{aligned} \tag{9}$$

Plug in Equation (9) back into $F(x)$,

$$F(x) = C_2 \sin(\frac{n\pi x}{L})\Bigg| \left\{ n \in \mathbb{Z}^+ \right\} \tag{10}$$

5.1.2 Solving the Time Dependent Differential Equation

One could observe that the time dependent equation in Equation (5) is highly similar in structure to the time independent differential equation we solved in Section 5.1.1. Thus from Equation (5) use the case of $k < 0$.

Let $k = -a^2 = -\frac{n^2\pi^2}{L^2}$ where a is solved in Equation (9). Substitute k into Equation (5).

$$\begin{aligned} \frac{d^2G}{dt^2}\frac{1}{G\nu} &= -\frac{n^2\pi^2}{L^2} \\ \frac{d^2G}{dt^2} &= -\frac{n^2\pi^2\nu}{L^2}G \end{aligned}$$

$$\begin{aligned} \frac{d^2G}{dt^2} + \frac{n^2\pi^2\nu}{L^2} &= 0 \\ G(\frac{d}{dt} + i\frac{n\pi\sqrt{\nu}}{L})(\frac{d}{dt} - i\frac{n\pi\sqrt{\nu}}{L}) &= 0 \end{aligned}$$

From here, one is able to get that

$$\frac{dG_1}{dt} = -i\frac{\sqrt{\nu}n\pi}{L}G_1$$

$$\frac{dG_2}{dt} = i\frac{\sqrt{\nu}n\pi}{L}G_2$$

Solve the above first order differential equation,

$$G_1 = e^{-i\frac{\sqrt{\nu}n\pi}{L}} \tag{11}$$

$$G_2 = e^{i\frac{\sqrt{\nu}n\pi}{L}} \tag{12}$$

Use Euler's equation to obtain $G(t)$ knowing that $G(t) = A'G_1 + B'G_2$,

$$G(t) = A\cos(\frac{\sqrt{\nu}n\pi}{L}t) + B\sin(\frac{\sqrt{\nu}n\pi}{L}t)\bigg| \left\{n \,\epsilon\, \mathbb{Z}^+\right\} \tag{13}$$

Note that A' and B' is included in both constants A and B.

5.1.3 Build the 1D Wave Function

Plug in both Equation (10) and Equation (13) into Equation (4).

$$y(x,t) = [A\cos(\frac{\sqrt{\nu}n\pi}{L}t) + B\sin(\frac{\sqrt{\nu}n\pi}{L}t)]\sin(\frac{n\pi x}{L})\bigg| \left\{n \,\epsilon\, \mathbb{Z}^+\right\} \tag{14}$$

Note that the constant term C_2 in Equation (10) is multiplied into the bracket and is a part of A and B. Based on the superposition principle, any sum of solutions is also a solution. Sum up all possible result from Equation (14) to find a series of solutions.

$$y(x,t) = \sum_{n=1}^{\infty}[A_n\cos(\frac{\sqrt{\nu}n\pi}{L}t) + B_n\sin(\frac{\sqrt{\nu}n\pi}{L}t)]\sin(\frac{n\pi x}{L}) \tag{15}$$

From the boundary condition, the initial speed of the string is 0.

$$v(x,t) = \frac{\partial y(x,t)}{\partial t} = \sum_{n=1}^{\infty}[-A_n\frac{\sqrt{\nu}n\pi}{L}\sin(\frac{\sqrt{\nu}n\pi}{L}t) + B_n\frac{\sqrt{\nu}n\pi}{L}\cos(\frac{\sqrt{\nu}n\pi}{L}t)]\sin(\frac{n\pi x}{L}) \tag{16}$$

Substitute $t = 0$ into Equation (16),

$$0 = v(x,0) = \sum_{n=1}^{\infty} B_n\frac{\sqrt{\nu}n\pi}{L}\sin(\frac{n\pi x}{L})$$

It should be obvious that $B_n = 0$.

Therefore, the final wave function is

$$y(x,t) = \sum_{n=1}^{\infty} A_n\cos(\frac{\sqrt{\nu}n\pi}{L}t)\sin(\frac{n\pi x}{L}) \tag{17}$$

5.2 The Ideal Pickup Location Based on the Wave Function

Let the location of the pickup to be P. Plug it into Equation (17).

$$y(P,t) = \sum_{n=1}^{\infty} A_n\cos(\frac{\sqrt{\nu}n\pi}{L}t)\sin(\frac{n\pi P}{L})$$

Thus, amplitude at P will be

$$A_n(P) = A_n \sin(\frac{n\pi P}{L}) \tag{18}$$

Let $P = \frac{L}{N}$, then substitute it into Equation (18),

$$A_n(\frac{L}{N}) = A_n \sin(\frac{n\pi}{N}) \tag{19}$$

In Equation (19), one could see that $A_n(\frac{L}{N}) = 0$ when $n = N$. This represents the physical phenomenal of a node. Let $N \to \infty$ if to preserve as many orders of harmonic as possible. Since P approaches 0 as $N \to \infty$, it is the best for the pickup to be placed as close to the bridge as possible. This corresponds to the brighter, clearer tone characteristic of the acoustic sasando.

A smaller amplitude at the pickup also provides greater headroom in the subsequent signal chain. Because each device has a maximum allowable voltage, keeping the input level lower ensures that more of the signal's dynamic range can be preserved without clipping, allowing for more flexibility during later processing.

6 Band-pass Filter

To modify the tone of the pickup signal and reproduce the authentic sound of the instrument, a band-pass filter will be applied to the pickup signal. The biquad band-pass is a second order linear recursive filter that can act equivalently to a damped harmonic oscillator. A digital implementation for this filter was chosen as it is easier to adjust bandwidth and resonance, avoids the need to add additional physical circuits for multiple resonances, and eliminates concern about the tolerance of physical components. By tuning the center frequency and quality factor, the digital biquad can effectively mimic the acoustic characteristics of the instrument.

The biquad transfer function is defined as:

$$H(z) = \frac{b_0 + b_1 z^{-1} + b_2 z^{-2}}{a_0 + a_1 z^{-1} + a_2 z^{-2}} \tag{20}$$

Using the definition of coefficients for the band-pass filter with constant 0 db peak gain preserves the conventional -3 dB passband and the natural dynamics of the volume (Bristow-Johnson, 2002).

$$\begin{aligned} b_0 &= \alpha \\ b_1 &= 0 \\ b_2 &= -\alpha \\ a_0 &= 1 + \alpha \\ a_1 &= -2\cos\omega_0 \\ a_2 &= 1 - \alpha \end{aligned} \tag{21}$$

where

$$\begin{aligned} \omega_0 &= 2\pi \frac{f_0}{F_s} \\ \alpha &= \frac{\sin\omega_0}{2Q} \end{aligned} \tag{22}$$

The filter is implemented using the Direct Form 1 implementation (Bristow-Johnson, 2002):

$$y[n] = \left(\frac{b_0}{a_0}\right) x[n] + \left(\frac{b_1}{a_0}\right) x[n-1] + \left(\frac{b_2}{a_0}\right) x[n-2] \\ - \left(\frac{a_1}{a_0}\right) y[n-1] - \left(\frac{a_2}{a_0}\right) y[n-2] \tag{23}$$

where $x[n]$ and $y[n]$ are the input and output audio samples, respectively. With multiple filters, the difference equation above can be summed in parallel to preserve independent resonances.

$$y[n] = y_1[n] + y_2[n] + y_3[n] + ... \tag{24}$$

6.1 Leaf Resonator

It is given that leaf resonator amplifies frequencies between 98 Hz and 1047 Hz. These values will be the upper and lower frequency limit of the filter: $f_L = 98$ Hz and $f_H = 1047$ Hz.

The center frequency and bandwidth are calculated from the upper and lower limit as:

$$\begin{aligned} f_0 &= \sqrt{f_L \cdot f_H} \\ &= \sqrt{98 \text{ Hz} \cdot 1047 \text{ Hz}} \\ &= 320.3217133 \text{ Hz} \\ &= 3.2 \times 10^2 \text{ Hz} \end{aligned}$$

$$\begin{aligned} BW &= f_H - f_L \\ &= 1047 \text{ Hz} - 98 \text{ Hz} \\ &= 949 \text{ Hz} \end{aligned}$$

The corresponding quality factor calculated using the center frequency and the bandwidth:

$$\begin{aligned} Q &= \frac{f_0}{BW} \\ &= \frac{3.2 \times 10^2 \text{ Hz}}{949 \text{ Hz}} \\ &= 0.3375360519 \\ &= 0.34 \end{aligned}$$

This low quality factor is consistent with the broad range of the overall resonance of the leaf resonator.

The sampling frequency F_s will be taken at the recommended standard of 48 kHz for audio production (Audio Engineering Society, 2018). This sampling frequency reduces the risk of aliasing from undersampling, and ensures that the filter will be compatible with modern audio software.

Using the values above, ω_0 and α values are calculated with Equations (22):

$$\begin{aligned}
\omega_0 &= 2\pi\frac{f_0}{F_s} \\
&= 2\pi\frac{3.2\times 10^2\text{ Hz}}{48\times 10^3\text{ Hz}} \\
&= 0.04193001422\text{ rad} \\
&= 0.042\text{ rad}
\end{aligned}$$

$$\begin{aligned}
\alpha &= \frac{\sin\omega_0}{2Q} \\
&= \frac{\sin 0.042}{2(0.34)} \\
&= 0.06209370627 \\
&= 0.062
\end{aligned}$$

Using Equations (21), the filter coefficients are then:

$$\begin{aligned}
b_0 &= \alpha \\
&= 0.062
\end{aligned}$$

$$b_1 = 0$$

$$\begin{aligned}
b_2 &= -\alpha \\
&= -0.062
\end{aligned}$$

$$\begin{aligned}
a_0 &= 1+\alpha \\
&= 1+0.062 \\
&= 1.062 \\
&= 1.1
\end{aligned}$$

$$\begin{aligned}
a_1 &= -2\cos\omega_0 \\
&= -2\cos(0.042) \\
&= -1.998242131 \\
&= -2.0
\end{aligned}$$

$$\begin{aligned}
a_2 &= 1-\alpha \\
&= 1-0.062 \\
&= 0.9379062937 \\
&= 0.94
\end{aligned}$$

To be implemented, these coefficients must be normalized by a_0. Doing so for all coefficients results in final coefficients of

$$\begin{aligned}
b &= [0.059, 0.0, -0.059] \\
a &= [1.0, -1.9, 0.88]
\end{aligned} \tag{25}$$

Taking these coefficients and inputting them into audio software using Equation (23) for real-time filtering of the pickup signal.

To verify the model response, a simulated input was fed to the filter function in MATLAB. Note that the code used is included in Appendix A.

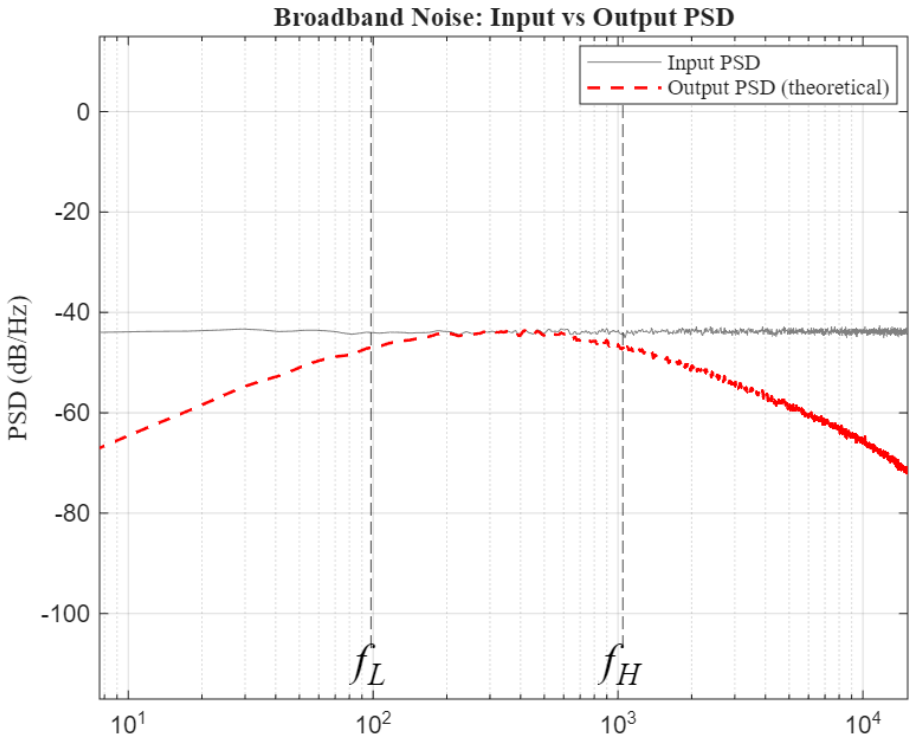

Figure 12: Response of the digital filter from a spectrum of randomized gaussian noise.

Figure 12 shows a power spectral density plot that exhibits a pronounced attenuation of frequency components outside the cutoff region, confirming that the filter effectively suppresses out-of-band content. For conciseness, the implementation code is omitted here and provided in Appendix A; it is fully annotated, so no additional explanation is required.

6.2 Bamboo Tube as Resonator

It is given that the bamboo tube of the sasando has a length of 70 cm and a diameter of 8 cm. Qualitative research suggest that the bamboo tube is closed on both ends.

For a closed tube standing waves with nodes at both ends, the wavelengths and resonant frequencies are:

$$\begin{aligned} \lambda_n &= \frac{2\ell}{n} \\ f_n &= \frac{v}{\lambda_n} \\ n &= 1, 2, 3... \end{aligned} \tag{26}$$

Using Equations (26) with $v = 343$ m/s as the speed of sound and taking $\ell = 0.7$ m, the first five wavelength and frequencies from $n = 1, 2, 3, 4, 5$ are:

n	λ_n	f_n
1	1.4	245
2	0.70	490
3	0.47	735
4	0.35	980
5	0.28	1225

It can be seen that the first 4 resonant frequencies of the bamboo tube falls within the resonance frequency range of the leaf resonator. This could mean the bamboo tube would also amplify these specific frequencies in addition to the amplification of the leaf resonator. To reproduce this, four filters corresponding to each frequency can be added.

The quality factor can be chosen based on the acoustic properties of the bamboo material. From Figure 13 with data by Liu et al. (2012), considering the lower moisture level of 8.25% and the average Indonesian temperature of 25°, the internal friction can be approximated to

$$\tan\delta = 0.053 \pm 0.005$$

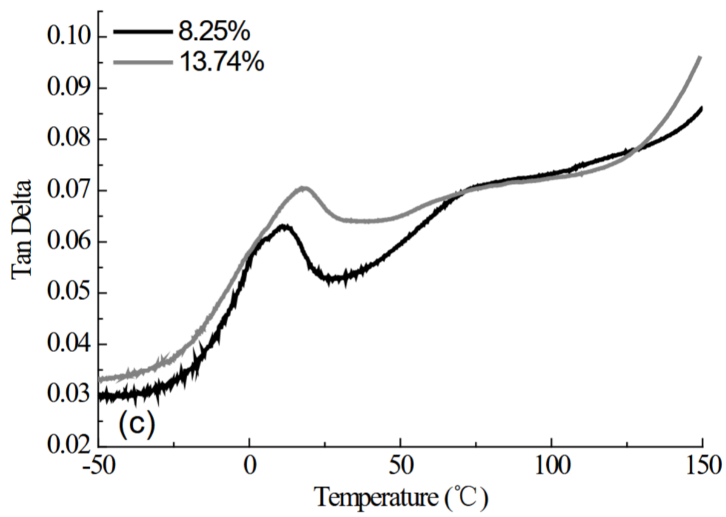

Figure 13: Internal friction of the internal section of bamboo as a function of temperature at moisture levels of 8.25% and 13.74%.
Note. Adapted from "Dynamic mechanical thermal analysis of moso bamboo (*Phyllostachys heterocycla*) at different moisture content," by Z. Liu, Z. Jiang, Z. Cai, B. Fei, Y. Yu, and X. Liu, 2012, *Bioresources, 7*. https://doi.org/10.15376/biores.7.2.1548-1557

Calculating for the quality factor based on the relation:

$$\begin{aligned} Q &= \frac{1}{\tan\delta} \\ &= \frac{1}{0.053} \\ &= 18.86792453 \\ &= 19 \pm 2 \end{aligned} \qquad \begin{aligned} \delta Q &= Q(\frac{\delta(\tan\delta)}{\tan\delta}) \\ &= 18.86792453(\frac{5\times 10^{-3}}{0.053}) \\ &= 1.77999288 \\ &= 2 \end{aligned}$$

The quality factor for the bamboo tube is calculated to be 19 ± 2.

Using uncertainty propagation, the uncertainty formulas for values needed can be calculated using standard formulas. The uncertainty formulas for α and an example for the uncertainty for a coefficient are:

$$\delta\alpha = \alpha\frac{\delta Q}{Q}$$

$$\delta b_0, \text{normalized} = \sqrt{(\frac{\delta\alpha}{b_0})^2 + (\frac{b_0\delta\alpha}{a_0^2})^2}$$

With the same process as the leaf resonator and including the uncertainty propagation for all coefficients, the final, normalized coefficients for each bamboo tube harmonic are:

1. 245 Hz

$$b = [8.4 \times 10^{-4} \pm 9 \times 10^{-5}, 0.0, -8.4 \times 10^{-4} \pm 9 \times 10^{-5}]$$
$$a = [1.0, -1.9972 \pm 2 \times 10^{-4}, 0.9983 \pm 1 \times 10^{-4}]$$

2. 490 Hz

$$b = [1.7 \times 10^{-3} \pm 2 \times 10^{-4}, 0.0, -1.7 \times 10^{-3} \pm 2 \times 10^{-4}]$$
$$a = [1.0, -1.9925 \pm 4 \times 10^{-4}, 0.9966 \pm 3 \times 10^{-4}]$$

3. 735 Hz

$$b = [2.5 \times 10^{-3} \pm 3 \times 10^{-4}, 0.0, -2.5 \times 10^{-3} \pm 3 \times 10^{-4}]$$
$$a = [1.0, -1.9857 \pm 5 \times 10^{-4}, 0.9950 \pm 4 \times 10^{-4}]$$

4. 980 Hz

$$b = [3.4 \times 10^{-3} \pm 4 \times 10^{-4}, 0.0, -3.4 \times 10^{-3} \pm 4 \times 10^{-4}]$$
$$a = [1.0, -1.9769 \pm 7 \times 10^{-4}, 0.9933 \pm 5 \times 10^{-4}]$$

These bamboo tube resonance coefficients along with those of the leaf resonator can build a robust digital filter that reproduces the authentic tone of the sasando.

7 Power Amplifier and Speaker

After the voltage signal has been processed with the appropriate tone control by the biquad filter, it needs to be processed by an audio amplifier to amplify the signal to be enough for driving loudspeakers, thus the projection of the acoustic sounds (Lähdevaara, 2012). There are three types of amplifiers, where Class AB is the most popular class used in audio amplifiers as it enhances the efficiency compared to class A and avoids non-linear distortion caused by class B amplifiers (Lähdevaara, 2012). Both positive and negative input voltage signals are enhanced partially in Class AB amplifiers, as seen in Figure 14.

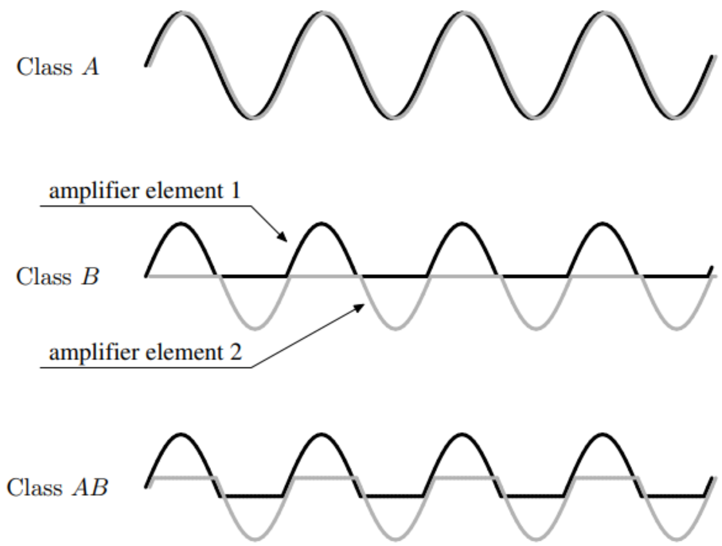

Figure 14: Comparison of the three classes of power amplifiers: A, B and AB. Note. Adapted from from *The science of electric guitars and guitar electronics*, by J. Lähdevaara (2012), Books On Demand. (OCLC: 861737010)

The difference between the input and output signals in the power amplifier is referred to as the gain of the amplifier, A, which can be defined as (Electronics-Tutorials, 2014):

$$A_v = \frac{V_{out}}{V_{in}}$$
$$A_i = \frac{I_{out}}{I_{in}}$$
$$A_p = \frac{A_v}{A_i}$$

The power gain, A_p, is defined as the multiplication of the voltage gain A_v and the current gain A_i. Power amplifiers in real life do not have perfect efficiency as some power would be lost to heat. The efficiency, η can be calculated based on the relationship below:

$$\eta = \frac{P_{out}}{P_{in}}$$

By using Class AB power amplifier the efficiency percentage is about 50 to 70% (Electronics-Tutorials, 2014).

The principle of an ideal amplifier model is to convert an external DC power supply into AC voltage signal that mirrors the input signal but amplified (Electronics-Tutorials, 2014). This signal would then be delivered to an output device like a speaker. Usually a moving-coil loudspeaker would be the most-common type of loudspeaker element for music instrument amplification (Electronics-Tutorials, 2014).

8 Strength and Weakness of Approach

8.1 Solution Summary

Our proposed model of an electric sasando to enhance its acoustic property is to use a system of optical pickups, one for each string, placed in the lower region and close to the bridge. Each optical pickup system would consist of a photointerruptor module (namely H21B1), which is an IR LED paired with a photo-transistor. Additionally, a digital biquad band-pass filter would be applied to the pickup signal to adjust bandwidth and resonance, a selector that simulates the leaf resonantor and amplifies the acoustic resonance frequencies between 98 Hz and 1047 Hz. Two converters are placed before the biquad filter (analog-to-digital converter) and after the biquad filter (digital-to-analog converter) respectively to convert between digital and analog signals. The resonance of the bamboo tube as a closed air column is also taken into consideration, where four extra biquad filters are added. Each filter corresponds to the resonance frequency that would be amplified by the leaf resonator. An overview of the final setup can be found in Figure 15.

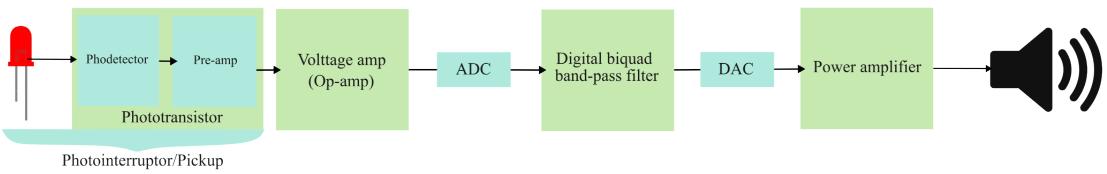

Figure 15: Overview of the final audio processing stream.

8.2 Strength of Approach

The strength of the approach is apparent compared to other possible solutions, for instance, having choice of pickups. Optical pickups are displacement-sensitive and highly resilient to interference due to change in electromagnetic field. It also captures the mechanical vibration of the strings, allowing it to capture the original acoustic characteristics of the string itself, as opposed to a 'spiced' set of amplitude spectrum using magnetic pickups. Furthermore, it allows for more options of the material of the string, as optical pickups are non-contact sensors and do not require interactions of the string with the pickup.

Using the biquad band-pass filter is effective in that it can be adjusted and set to amplify the same set of frequencies that the leaf resonator would be amplifying in a traditional sasando. This is a key filter that is lacking in current models of electric sasando, where the main goal is simply to amplify sounds, sacrificing the acoustic quality. Applying the filter could re-create the leaf resonator electronically. Using a digital biquad filter would also offer shielding from external noise and flexibility in altering characteristics to fit different sasandos as digital filters are programmed instead of relying on hardware.

8.3 Weakness of Approach

The weakness of the approach mainly lies in the complexities with independent systems per string. In the context here only the gong sasando is considered, which is known to have only 9 to 11 strings (Bakok, 2014). However, there are other variations of sasando which have far more numbers of strings. For instance, the violin sasando, which produces diatonic tones, has 32 to 36 strings (Bakok, 2014). If optical pickup were still to be used for a violin sasando, the number of pickups that need to be installed increase significantly, leading to potential high costs of manufacturing. Especially if every optical pickup were to be placed near the bridge, whose position varies for each individual string, the potential error due to the complexity of the system would become non-negligible. Furthermore, optical pickup is a type of active pickup where a DC power supply must be connected to power the optical systems and generation of voltage signals, this would likely cause inconvenience compared to other passive pickups such as magnetic or piezoelectric pickups.

Last but not least, using the digital biquad filter would create latency issues. Analog circuits are continuous and spontaneous, whereas a digital circuit only takes in discrete values and thus voltage signals from the optical pickup needs to be resolved into discrete steps by the analog-to-digital converter (ADC) (Lähdevaara, 2012). Depending on the ADC technology used, there is a tradeoff between the speed of resolving (sampling frequency) and the resolution (the number of steps in total). With audio amplifications in music performance, sampling frequency of an ADC needs to be considerably faster to minimize latency. Such choice of technology however, would often sacrifice resolution which could potentially cause signal distortions. The same applies to digital-to-analog converter (DAC). Thus using a digital filter instead of an analog filter might have latency issues as a disadvantage.

9 Conclusion

In this paper a potential model to enhance current electric sasando designs to recover the acoustic quality is discussed. Our solution is based on capturing the resonating and amplifying property of the lontar leaf resonator via digital biquad band-pass filter, as well as selecting an optical pickup system to avoid distortion of tone.

Based on analysis of principles of different pickups, we concluded that an optical pickup system is the most effective transducer that would minimize distortion of the acoustic quality of the string vibrations. This pickup choice is not susceptible to electromagnetic hum and would provide a less invasive approach of installation. It is also concluded from our derivation of the wave equation in relation to pickup position P, that the optimal location for the optical pickup is in near proximity of the bridge, approaching the bridge from below.

For the primary digital biquad filter, the quality factor Q to replicate the frequency amplification range of the lontar leaf is calculated to be $Q \approx 0.34$. The coefficients of the transfer function for the digital filter are calculated to be $b = [0.059, 0.0, -0.059]$ and $a = [1.0, -1.9, 0.88]$. The resonance caused by the closed air column created by the hollow bamboo tube is also put into consideration, where the specific harmonic order frequency that should be amplified are calculated to be: 245 Hz, 490 Hz, 735 Hz and 908 Hz. The related quality factor is $Q \approx 19 \pm 2$ based on the internal friction of the bamboo tube. The entire model of signal processing starts with the photointerruptor module (which consists of the IR LED and the phototransistor), then the operational amplifiers that further amplifies the voltage signal, after that the ADC which converts the analog signal to a digital signal. The digital signal gets filtered in the arrays of biquad band-pass filters, after that the processed signal gets converted back to an analog signal to be sent to a Class AB power amplifier, and finally the signal gets broadcasted and translated into mechanical sound.

This approach, while preserving the acoustic quality, has practical trade-offs. The primary disadvantages are the latency and signal distortion due to the analog-to-digital conversion required for a digital biquad filter. There is also additional complexity to the system of implementing optical pickups when the sasando has a relatively high string count, primarily because each string has to be paired with one optical pickup system. Despite these limitations, it still serves to be a flexible method to preserve the unique acoustic quality of a traditional sasando.

References

Audio Engineering Society. (2018). *Aes recommended practice for professional digital audio – preferred sampling frequencies for applications employing pulse-code modulation* (AES Standard No. AES5-2008). Audio Engineering Society. (Retrieved 2010-01-18)

Bakok, Y. D. B. (2014). Electric sasando of east nusa tenggara, indonesia. , *1*(2), 84–93. Retrieved 2025-11-08, from https://journal.isi.ac.id/index.php/IJCAS/article/view/1562 doi: 10.24821/ijcas.v1i2.1562

Bera, B. (2016). Piezoelectric effect, piezotronics and piezophototronics: A review. *Imperial Journal of Interdisciplinary Research (IJIR)*, *2*. Retrieved 2025-11-08, from https://www.academia.edu/37599716/Piezoelectric_Effect_Piezotronics_and_Piezophototronics_A_Review

Bristow-Johnson, R. (2002). *The audio eq cookbook*. https://webaudio.github.io/Audio-EQ-Cookbook/audio-eq-cookbook.html. (Accessed: 2025-11-08)

Electronics-Tutorials. (2014). *Introduction to the amplifier.* https://www.electronics-tutorials.ws/amplifier/amp_1.html. (Accessed: 2025-11-09)

ElProCus. (n.d.). *Preamplifier : Circuit, working, types, differences, how to choose, its application.* https://www.elprocus.com/preamplifier/. (Accessed: 2025-11-08)

Englert, P. W. (2018). *Analysis of current electric pickup technology utilized in clarinet performance and investigation into potential improvements* (Unpublished doctoral dissertation). Arizone State University.

Gautschi, G. (2002). *Piezoelectric sensorics*. Springer. Retrieved 2025-11-08, from http://link.springer.com/10.1007/978-3-662-04732-3 doi: 10.1007/978-3-662-04732-3

Hanson, R. J. (1987). Optoelectronic detection of string vibration. *The Physics Teacher*, *25*, 165–166.

Horton, M. T., N.G. (2009). Modeling the magnetic pickup of an electric guitar. *American Journal of Physics*, *77*, 144–150.

Kubilary, I. A. (2018, September). Optical pickups for string musical instrument. In *International conference on science and technology.*

Liu, Z., Jiang, Z., Cai, Z., Fei, B., Yu, Y., & Liu, X. (2012, February). Dynamic mechanical thermal analysis of moso bamboo (phyllostachys heterocycla) at different moisture content. *Bioresources*, *7*. doi: 10.15376/biores.7.2.1548-1557

Lähdevaara, J. (2012). *The science of electric guitars and guitar electronics*. Books On Demand. (OCLC: 861737010)

Mathews, M. V. (1988). *Pickups for the vibrations of violin and guitar strings using piezoelectric bimorphic bender elements* (Tech. Rep.). Stanford University, Center for Computer Research in Music and Acoustics (CCRMA).

Mustonen, M., Kartofelev, D., Stulov, A., & Välimäki, V. (2014, July). Experimental verification of pickup nonlinearity. In *International symposium on musical acoustics.*

Red Lion Controls, I. (2000, August). *Magnetic pickups in-line preamplifier — bulletin no. mp-h* (Technical Report No. MP-H). Retrieved from https://www.farnell.com/datasheets/2058061.pdf (Drawing No. LP0020; Revised 8/00; available online)

Tukan, M. K. A. C. S. D., Ceunfin, F., & Kian, M. (2020). How to play and tune sasando in edon style. , *22*(1), 21–36. Retrieved 2025-11-08, from https://www.neliti.com/publications/384544/ (Publisher: Indonesian Institute of the Arts, Padang Panjang) doi: 10.26887/ekspresi.v22i1.1038

Appendices

A Code used for Figure 12

Below is the code for Figure 12 written in MATLAB.

```
%RBJ BPF 98  1047  Hz @ 48 kHz
clear; clc;

Fs = 48000; % standard sample frequency as mentioned before
fL = 98; fH = 1047;
f0 = sqrt(fL*fH);
BW = fH - fL;
Q  = f0 / BW;

w0    = 2*pi*f0/Fs;
cw0   = cos(w0);
sw0   = sin(w0);
alpha = sw0/(2*Q);

b = [alpha, 0, -alpha];
a = [1 + alpha, -2*cw0, 1 - alpha];
b = b / a(1); %normalize them
a = [1, a(2)/a(1), a(3)/a(1)];

Nresp = 16384;
[H, f] = freqz(b, a, Nresp, Fs); %evaluate transfer function using the MATLAB toolbox

figure(1); clf;
semilogx(f, 20*log10(abs(H)+eps), 'LineWidth', 1.4); grid on;
xlim([20 20000]); ylim([-60 6]);
xlabel('Frequency (Hz)'); ylabel('Magnitude |H(f)| (dB)');
title(sprintf('RBJ Band-Pass (%.0f  %.0f Hz), f0=%.2f Hz, Q=%.3f, Fs=%g kHz', ...
              fL, fH, f0, Q, Fs/1000));
yl = ylim; hold on; plot([fL fL], yl, 'k--'); plot([fH fH], yl, 'k--');

%generate gaussian noise for 8s with a set seed
N = Fs * 8;
rng(0);
x = randn(N,1);
y = filter(b, a, x); %implement our filter with the precalculated a and b

%estimate input with Welch toolbox
win   = hamming(4096, 'periodic');
nover = round(0.5*numel(win));
nfft  = 8192;

[Px, fx] = pwelch(x, win, nover, nfft, Fs, 'psd');
Px_dB = 10*log10(Px + eps);

% Theoretical output PSD = input PSD + 20*log10(|H(f)|)
H_fx   = freqz(b, a, fx, Fs);
Py_the = Px_dB + 20*log10(abs(H_fx) + eps);
```

```
% plot the input vs output
figure(2); clf;
semilogx(fx, Px_dB, 'Color', [0.5 0.5 0.5]); hold on;

semilogx(fx, Py_the, 'r--', 'LineWidth', 1.2);
grid on; xlim([20 20000]); ylim([-140 -20]);
xlabel('Frequency (Hz)'); ylabel('PSD (dB/Hz)');
title('Broadband Noise: Input vs Output PSD');
legend('Input PSD', 'Output PSD (theoretical)','Location','SouthWest');
yl = ylim;
hL = xline(fL,'k--','f_L', 'Interpreter','tex', ...
           'LabelVerticalAlignment','top',  ...
           'LabelOrientation','aligned',    ...
           'HandleVisibility','off');
hH = xline(fH,'k--','f_H', 'Interpreter','tex', ...
           'LabelVerticalAlignment','top', 'LabelOrientation','aligned', ...
           'HandleVisibility','off');
```